Testing the efficacy of a Mars submillimeter (submm) sounder for atmospheric measurements

L. K. Tamppari, *Jet Propulsion Laboratory/California Institute of Technology, Pasadena, CA, USA (leslie.tamppari@jpl.nasa.gov),* **N. J. Livesey, W. Read** *Jet Propulsion Laboratory/California Institute of Technology, Pasadena, CA, USA,* **D. Banfield,** *NASA Ames Research Center, Moffett Field CA, USA,* **B. Ward,** *Flatiron Institute, New York, NY, USA,* **F. Forget, E. Millour,** *Laboratoire de Météorologie Dynamique, Paris, France,* **L. Steele,** *European Centre for Medium-Range Weather Forecasts, Reading, UK,* **M. Kahre,** *NASA Ames Research Center, Moffett Field CA, USA,* **R. Haberle,** *Capitola, CA, USA,* **G. Chattopadyay, D. Hayton,** *Jet Propulsion Laboratory/California Institute of Technology, Pasadena, CA, USA,* **P. Hartogh,** *Max Planck Institute for Solar System Research, Göttingen, Germany.*

Introduction: The study of the Martian atmosphere has advanced significantly over the last 30 years, however, daily, global measurements of winds and water vapor have not been obtained, yet are crucial for understanding vapor transport, illuminating the role of water-regolith interaction, and quantifying the large-scale circulation and wave activity that are present in the current climate on Mars. Furthermore, understanding the current climate and being able to constrain global circulation models (GCMs) are necessary for accurately evaluating scenarios for the past Martian climate, during a time when it was vastly different and likely had flowing liquid water and possibly microbial life.

Here we describe our efforts to construct the key components of an end-to-end *Observing System Simulation Experiment* (OSSE) suitable for quantifying the potential scientific value of vertically resolved wind and water vapor observations of the Martian atmosphere from an orbital vantage point. OSSEs, originally developed for quantifying the benefits of potential new Earth meteorological observations, are increasingly used to measure the potential utility of observation concepts across a wide range of disciplines. An end-to-end OSSE comprises a truth data set (such as GCM output) often known as the "nature run", a synthetic instrument data set sampled from the truth data set, the capability to infer atmospheric phenomena from both, and evaluation of the ability of the putative measurements to answer scientific questions. We recognize that, as for many others, our approach stops short of a full OSSE which, in its original form, includes work to assimilate observations, or in some cases radiances, into a model. Accordingly, we refer to our process as a pseudo-OSSE.

In our pseudo-OSSE, we assess the efficacy of a submm sounder [1] capable of retrieving vertical profiles of water vapor, winds, and temperature to reproduce the "true" atmospheric fields provided by the LMD GCM. Our objective is to determine how well the simulated measurements are able to match the input data, giving insight into the ability of the submm instrument to answer outstanding scientific questions and to identify potential improvements to the instrument and/or its measurement strategy. Having a system to generate and compare simulated measurements to "truth" input allows for future assessments of various sampling strategies, orbital patterns, or instrument configurations and identification of those optimal for addressing a variety of science questions.

Methods: We assumed that the submm instrument would be flown on a spacecraft orbiting Mars at ~300 km altitude, with a 92° inclined, sun-synchronous, near-circular orbit, with an ascending nodal time of 3 p.m. We chose this orbit because it is similar to orbits that have been used for MRO and MGS, and would allow for qualitative comparisons to published data acquired from those spacecraft (e.g., water vapor column abundances from TES).

We assumed the instrument would have two identical instrument assemblies, each consisting of a 2-axis scanning telescope, a submm receiver, spectrometer, and associated electronics, and that each telescope would have both vertical and azimuthal scanning capability. We initially chose to examine an azimuthal sampling pattern in which one antenna was continuously pointed such that the line of sight is oriented south-to-north at the measurement location, and the other was continuously steered such that the line of sight is oriented west-to-east at the measurement location. This pointing was chosen to simplify the evaluation of the zonal and meridional winds. This sampling pattern, using the current sampling frequency, produced some unsampled latitude bands near the southern pole. We assume a vertical scan from the surface to 150 km over 76 sec. This provides a sampling frequency of one sample roughly every 4° on a great circle.

We evaluated the submm single-profile precisions and vertical for wind as a function of varying amounts of water vapor (Fig. 1). Because all available emission lines are used in combination to retrieve all quantities of interest (temperature, winds, water vapor), the precision due to the varying water vapor can affect precisions of the other retrieved quantities as well, though to a far smaller extent.

Results:

Wind and Temperature evaluation. We started with an evaluation of seasonally varying zonal-mean

zonal wind cross-sections and stationary wave phases and amplitudes. The ability of the simulated measurements to yield accurate and detailed information about these atmospheric dynamical processes was evaluated against similar analysis of the complete, regular latitude/longitude gridded, full time-resolution, un-averaged and noise-free data from the GCM to quantify the simulated instrument's ability to capture these scientifically important phenomena. These analyses follow from the work of Banfield et al. [e.g., 2-4].

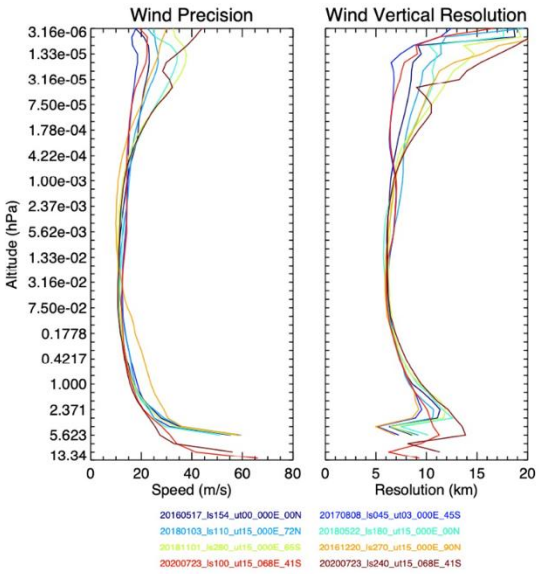

Figure 1. Wind retrieval single-profile precisions (left) and vertical resolutions (right) for varying water column abundances.

In Figure 2, the panels show the comparison between the LMD GCM and the synthetic data for the zonal means of temperature, zonal wind, and meridional wind for a Mars month of data in late northern winter. The overall temperature structure agrees quite well, but there are locations where the synthetic observations are off by about 5K. The zonal-mean zonal wind structure also agrees quite well, except that the chosen cadence of observations causes a latitudinal data gap in the polar vortex location at that season. Consequently, the position of this jet stream is well-estimated (from the temperatures and using the thermal wind equation), but the zonal winds are not directly measured in the jet itself. This insight is valuable and argues in favor of choosing other steering/scanning strategies, such as a more rapid scan to achieve denser latitudinal coverage. The zonal-mean meridional wind shows a relatively poor match, not only in magnitudes, but also in overall meridional structure. The cause of this discrepancy may be due to the sampling pattern and further investigation would assess this by examining a variety of patterns.

The wavenumber 2 stationary wave results (Figure 3) exhibit the same latitudinal gaps as the zonal mean results, but in general have overall better agreement with the LMD GCM. In all cases, a gap was apparent in the wind results for Z<1H (i.e., the bottom scale height of the atmosphere). This is a result of the poorer quality of the wind information in this region as shown in Fig. 1.

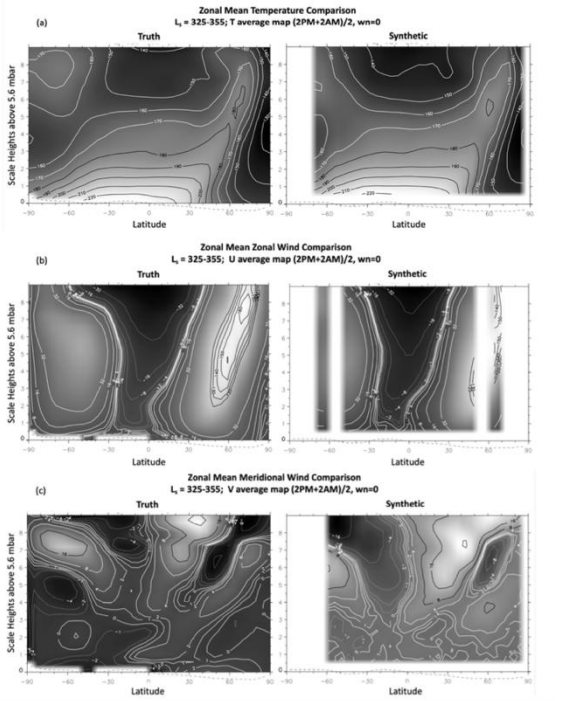

Figure 2. Comparison between the LMD GCM (left column, labeled "Truth") and the L2 synthetic data (right column) for the zonal means of temperature (a), zonal wind (b), and meridional wind (c). Note that gaps in the data result from the directly east-west and directly north-south views that were assumed in generating the synthetic data set (b and c, respectively; for a both are used).

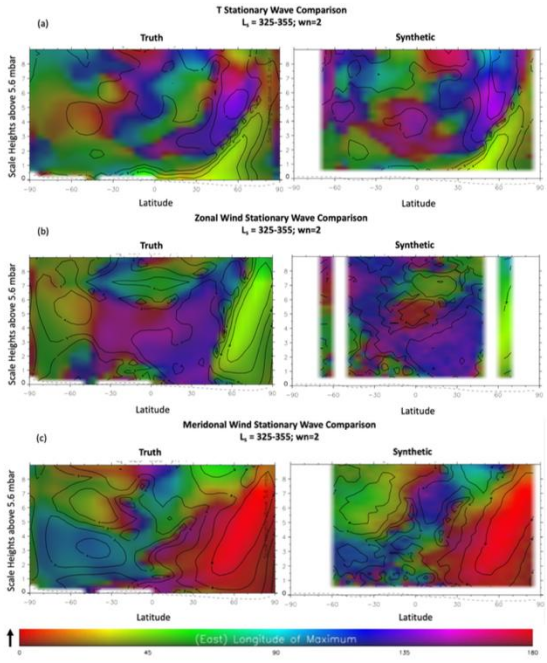

Figure 3. Comparison between the LMD GCM (left column, labeled "Truth") and the L2 synthetic data (right column) for the zonal mean wavenumber 2 stationary wave as reflected in amplitude (contours) and East longitude of maximum (hue; scale bar at bottom) for temperature (a), zonal wind (b), and meridional wind (c).

Water vapor evaluation: Our first comparison was to create a representation of the annual water cycle (Fig. 4) in both the LMD GCM output and the synthetic data. Our goal was to determine if the submm sounder could adequately reproduce the water vapor column abundances throughout the annual water cycle.

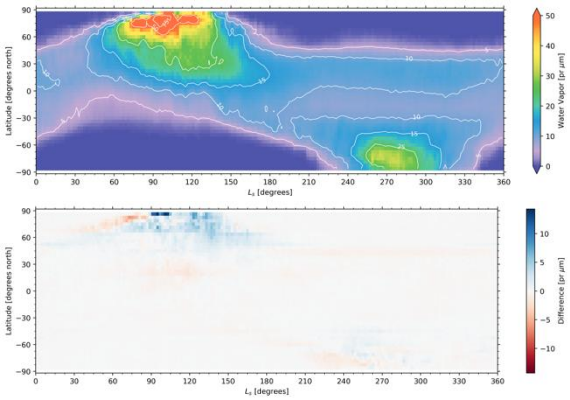

Figure 4. Seasonal zonally-averaged water vapor column abundances from the synthetic L2 data (top). (Bottom) Absolute difference in water vapor abundance, in pr μm, between the LMD GCM and synthetic data. The differences are generally <5%, even with the absolute differences are largest.

We also examined how well we could reproduce the spatial distribution of the water vapor as a function of season (Figures 5, 6).

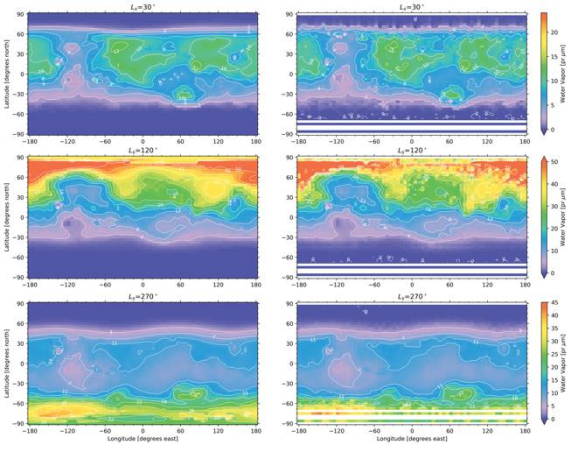

Figure 5. Seasonal snapshots of the spatial distribution of water vapor column abundances. The left column shows LMD GCM output and the right column shows the synthetic data. The top row shows the average column abundances in 3.75° x 5.625° lat/lon bins (the LMD output resolution) for a 30° seasonal window, centered at L_s = 30°, which represents the driest season planet-wide. The middle row shows similar plots for L_s = 120°, which represents the annual maximum in atmospheric water vapor column abundances. The bottom row shows similar plots for L_s = 270°, which represents the annual maximum atmospheric water vapor column abundances in the south polar region. Note the vapor abundance color scale bar changes for each row. The water vapor abundances are not scaled for surface pressure, in order to highlight the changing amounts with season and location.

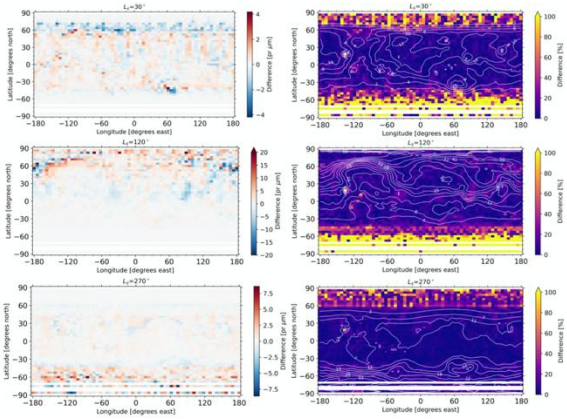

Figure 6. Seasonal snapshots of the spatial distribution of water vapor column abundances shown in Fig. 5. The left column shows absolute difference between the LMD GCM and the synthetic data, and the right column shows the percent differences between them. Note that the absolute difference scale bar (left column) changes by row. The top row shows the results for the L_s = 30° window, the middle row shows the results for the L_s = 120° window, and the bottom row shows the results for the L_s = 270° window. White contours show the column abundances.

It is also of interest to evaluate whether or not the submm instrument would be able to determine the timing of the seasonal global as well as hemispheric maximum and minimum water vapor in the system to within 5° L_s, to identify any interannual changes that may occur, and to reproduce both the magnitude of the total vapor as a function of season as well as its hemispheric distribution. [5] showed that there was interannual variability in the yearly peak of the water vapor abundances of about 0.1 x 10^{15} g and the seasonal date of that peak varied by 30-40° L_s centered around L_s = 120°. The LMD GCM shows the annual water cycle peak closer to L_s = 100°. Figure 7 shows that the synthetic L2 data do a very good job representing the LMD GCM. The curves are within 4% in all cases, and outside of the L_s = 120-150° season they are within ~1-2%, so determining the seasonal total and hemispheric abundance maxima and minima and timing is achievable.

We examined the LMD GCM and synthetic data vertical water vapor magnitude and distribution for the same three 30° seasonal periods as before: L_s = 30°, 120°, and 270° (Fig. 8). The zonally-averaged synthetic data for each seasonal period examined are

very similar to the LMD GCM, with latitudes and altitudes of water vapor mass mixing ratios matching well. The maximum absolute difference between the LMD and the synthetic data is $8x10^{-5}$ kg/kg, which occurs for annual maximum water vapor abundance of 0.001 kg/kg in the high northern latitudes, at low altitude, during northern summer. This is equivalent to an 8% difference. When vapor mass mixing ratios are extremely small, which occurs in the polar regions during dry conditions and at high altitudes, differences can be up to 100%.

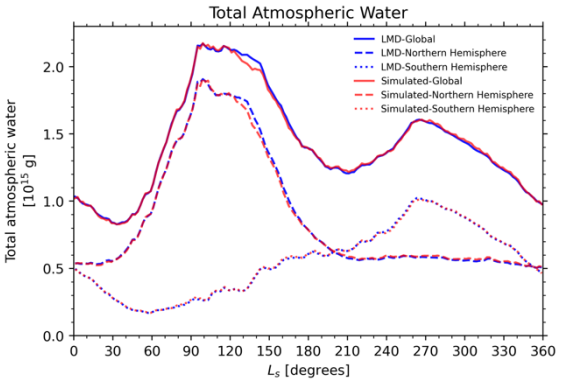

Figure 7. (Top) Total atmospheric water vapor abundance (solid line) as a function of season and separated by northern (dashed line) and southern (dotted line) hemispheres as a function of season for the LMD GCM (blue) and synthetic L2 data ("simulated" shown in red). Cf. Smith (2002), Figure 8. (Bottom) Percent difference between LMD GCM and synthetic L2 total global atmospheric water vapor abundances.

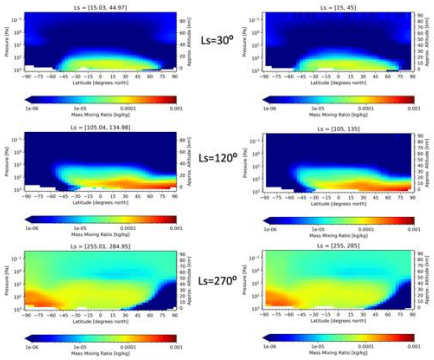

Figure 8. Zonally-averaged vertical distribution of water vapor mass mixing ratio for three 30° seasonal periods: (top row) L_s = 30°, planet-wide dry season, (middle row) L_s = 120°, northern hemisphere vapor maximum, and (bottom row) L_s = 270°, S hemisphere vapor maximum. The left column shows the LMD GCM output and the right column shows the synthetic L2 data.

We also examined the ability of the submm to reproduce the zonal-mean vapor mass stream function. Figure 9 shows this for the LMD and the synthetic data sets for the early northern summer time period, near the water vapor column maximum for the year. The mass stream function contours compare well, with a slightly higher estimate in the L2 synthetic data. This may result from the finer vertical gridding used in the L2 synthetic data set, the lat/lon gridding, and/or the fact that there are fewer time steps in the L2 data used (2deg L_S, whereas the LMD is averaged out to once-per-day).

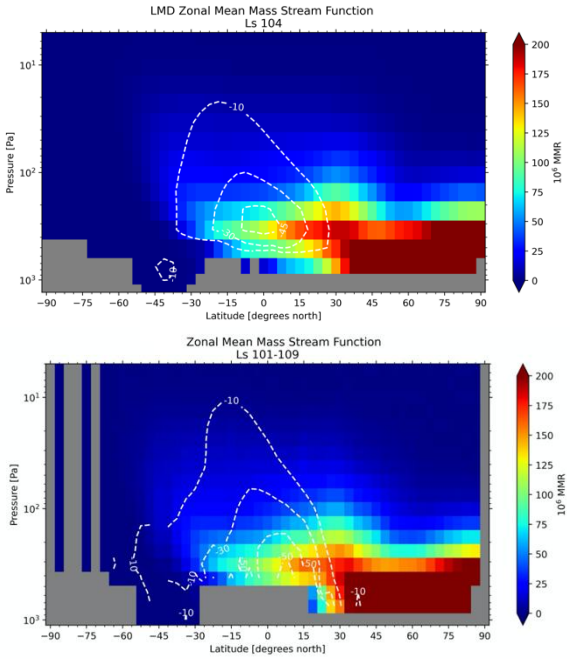

Figure 9. The zonal-mean vapor mass stream functions (contours) for the LMD data (top) and the synthetic data (bottom) in units of 10^8 kgs^{-1} (white, dashed contours). In each case, the water vapor mass mixing ratios are shown as well, in color.

Conclusions and Future Work: We have constructed key components of an end-to-end Mars OSSE and have demonstrated the efficacy of a two-antenna submm instrument for measuring vertical profiles of temperature, winds, and water vapor from an orbital platform. The pseudo-OSSE we have developed (process ends prior to full assimilation) demonstrates the framework on which future instrument evaluation/optimization could be conducted.

Our results show that a submm instrument, operating in a near-sun-synchronous orbit, would provide temperature, wind, and water vapor profiles with accuracy sufficient to measure key aspects of the martian atmosphere, many of which have not been measured or have been insufficiently measured, such as the strength of the zonal jets and a seasonal & global picture of water vapor vertical distribution.

This initial analysis is valuable to direct future efforts for improvement. Ensuring adequate coverage of the high latitudes is among the top priorities and could be improved by scanning a smaller altitude range. This could be evaluated in combination with a slower (faster) scan speed to determine if relatively higher (lower) precision is required balanced against latitudinal sampling (a faster scan speed for a given altitude range would yield more frequent latitudinal

sampling). In addition, specialized scanning patterns could be evaluated.

Bibliography: [1] Read et al., 2018. [2-4] Banfield et al., 2000, 2004, 2019. [5] Smith 2002.